Heliyon

ELSEVIER

Viability Test Device for anisakid nematodes

Michael Kroeger [a],[*], **Horst Karl** [b], **Bernhard Simmler** [a], **Peter Singer** [a]

[a] *technet GmbH, Pestalozzistraße 8, D-70563 Stuttgart, Germany*

[b] *Max Rubner-Institut, Palmaille 9, D-22767 Hamburg, Germany*

[*] Corresponding author.

E-mail address: michael.kroeger@technet-gmbh.com (M. Kroeger).

Abstract

Up to now the visual inspection of mobility of isolated anisakid larvae serves as a measure of viability and possible risk of infection. This paper presents a new method to rule out unreliability — caused by the temporary immobility of the larvae and by the human uncertainty factor of visual observation. By means of a Near infrared (NIR) imaging method, elastic curvature energies and geometric shape parameters were determined from contours, and used as a measure of viability. It was based on the modelling of larvae as a cylindrical membrane system. The interaction between curvatures, contraction of the longitudinal muscles, and inner pressure enabled the derivation of viability from stationary form data. From series of spectrally signed images within a narrow wavelength range, curvature data of the larvae were determined. Possible mobility of larvae was taken into account in statistical error variables. Experiments on individual living larvae, long-term observations of *Anisakis* larvae, and comparative studies of the staining method and the VTD measurements of larvae from the tissue of products confirmed the effectiveness of this method. The VTD differentiated clearly between live and dead nematode larvae isolated from marinated, deep-frozen and salted products. The VTD has been proven as excellent method to detect living anisakid nematode larvae in fishery products and is seen as useful tool for fish processing industry and control authorities.

Keywords: Biophysics

1. Introduction

Anisakid nematode larvae can be found in a large variety of marine fish species of commercial interest worldwide (Mattiucci and Nascetti, 2008). Most larvae are situated in the viscera but some individuals also penetrate into the surrounding fish muscle (Levsen and Lunestad, 2010). The consumption of living anisakids in raw or insufficiently prepared seafood products can lead to serious illness. This illness is known as intestinal anisakiasis, and is caused by drilling into the human gastric mucosa wall. It can also lead to allergic reactions among sensitised persons (Nieuwenhuizen and Lopata, 2013).

For this reason it is very important to check the viability of anisakids in fishery products.

In the pharmaceutical and medical fields, the determination of viability provides a component to assess the effectiveness of medication or therapeutic measures (Davey, 2011). In the area of foodstuffs, it has a comparable importance for checking products or manufacturing processes, in order to exclude health risks from contamination from living organisms (e.g. parasites or bacteria).

Viability is characterised by reproduction and metabolism (Schrödinger, 1944; Butler et al., 2014). The viability of microorganisms is essentially determined by measuring their reproduction rate. These measurements can be conducted quickly and cheaply with automated methods (plate count method) and are among the standard procedures in the area of medicine (Maturin and Peeler, 2001; Sutton, 2011; Moon et al., 2013).

Methods based on reproduction rates cannot be used to determine the viability of anisakid parasites such as *Anisakis simplex s.s.*, *Anisakis pegreffii* or *Pseudoterranova decipiens*. These organisms reproduce in the stomach chambers of living mammals (whales, common seals, grey seals), thus excluding examinations that are comparable with the plate count method.

To estimate the viability of anisakids, these are isolated from the fish tissue (Karl et al., 2014; Llanera-Reino et al., 2013) and examined visually by experts in accordance with valid regulations on food inspection. These methods are based on the classification of the mobility of larvae (Codex Stan 244, 2004; Giarratana et al., 2012, 2017; Hirasa and Takemasa, 1998; Karl et al., 2014; Oh et al., 2014; Pascual et al., 2010), susceptibility to staining (staining method) (Leinemann and Karl, 1988), or drilling properties (drilling method) (Priebe et al., 1973).

All the methods are based on visual observation by experts. Unreliable results are inherent because slow movements may not be recognised (Wertheimer, 1912; Giese and Poggio, 2003), and live nematodes may remain in a temporary motionless

state for several hours (Codex Stan 244, 2004; Milligan, 2008). Low colour differences or small drilling distances may not be recognised either (Biedermann, 1985) and not all live nematodes penetrate quantitatively into the agar if the drilling method is applied. Some remain on the surface.

Consequently, the actual viability tests to prove the safety of fishery products processed under conditions applied in the European fish industry are not sufficient, since their results based on subjective observations by experts which are not checkable and thus lead to discussions in good manufacturing practices (GMP) audits (Posset et al., 2017).

The aim of this study was to develop and to evaluate a Viability Test Device (VTD) which can be used to determine viability by classifying the shape characteristics of anisakid organisms independently of movement by transferring the differential-geometric approach of shape energy from the area of membrane biophysics to nematode larvae (Deserno, 2014). Based on the membrane approach a measuring system for a rapid retrieval of deformation and curvature data was to be developed.

The suitability of the membrane model was to be tested in individual studies, including a long-term monitoring of freshly isolated live *Anisakis* larvae over 4 weeks. Additionally, the performance capability of the Viability Test Device was also to be evaluated by means of comparative studies of nematode larvae from marinated, salted and deep-frozen herring products.

2. Background

2.1. Modelling of nematode larvae

In the biological literature, nematode larvae are described as elongated flexible membrane tube systems composed of a fibre matrix system of different layers. Helical crossed fibres limit the maximal inner volume (Goriely and Tabor, 2013; Clark and Cowey, 1958). Its cross-section is circular along the entire body (Grabda, 1991; Lucius and Loos-Frank, 2008). The inner tube is the carrier of basal metabolic activity. During its life status the outer tube is under constant mean inner pressure generated by the activity of the inner tube (Harris and Crofton, 1957).

Bending, stress and inner pressure of the tube are the governing features for viability measurement. These interacting features are used for modelling shapes and shape fluctuations. A relationship between the form and the metabolic activity of a larvae is generated by measuring its curvature properties. Because of the circular cross-section of the larvae, the elastic surface energy is determined from its experimentally accessible contour. Surface energy is assumed to be a mirror of the metabolic activity and viability of the organism.

The nematode model as a long closed cylindrical high flexible membrane tube is the basis for the operation of the Viability Test Device (VTD). By deformation analysis of the contour of the model parasite, its surface energy is minimized via a suitable parametrization and parameter variation. This results in the shape energy F (Eq. (1)) as a function of the radii of curvatures of all contour points (Sommerfeld, 1950; Helfrich, 1973; Zhong-can and Helfrich, 1989; Leibler, 2004):

$$F = \frac{1}{2}k_c \oint (c_1 + c_2 + c_0)^2 dA + \Delta p \int dV + \lambda \oint dA \qquad (1)$$

k_c represents the bending stiffness of the tube, Δp the pressure difference of the tube and surrounding medium and λ the tensile stress. dA refer to the surface area elements and dV to the volume elements, c_1 and c_2 refer to the principal curvatures of the membrane surface. The spontaneous curvature c_0 is caused by different material properties of multiple layers (Khairy and Howard, 2011; Svetina et al., 2004). In addition to the bending deformations, deformations of the surface and the volume have to be supplemented to the total energy. The total shape energy is obtained by minimizing F by varying the Lagrange multipliers Δp and λ (Zheng and Liu, 1993).

2.2. System design

Experimental access to the viability of single larvae and group of larvae (10−20 individuals) is achieved by multiple capture of their contours in image series and the subsequent calculation of form energies for all the single images. Within the time interval of an image series the volume and the cross section, the bending stiffness and the internal pressure of all identified objects are assumed to be constant. The VTD is intended to determine the viability of single larvae or of group of larvae up to 20 individuals, including their spatial and temporally changing mobility after isolation from the fish tissue and transferring them to a pepsin/HCL solution. When a live Anisakid larvae is placed in a pepsin/HCL solution at room temperature it shows typical movements whereas motionless larvae are considered from human observer to be dead. Our observations have shown that typical wriggling movements of nematode larvae were mainly parallel to the liquid surface in a petri dish (Fig. 1b) due to the low liquid height (Pepsin/HCL, approx.5 mm). The error caused by the deviation

Fig. 1. Contour images of a single object and two crossed objects (a), overlapping object ensemble (b).

from the preferred plane in the determination of curvatures is minimal. Therefore a time- and cost-intensive 3D measurement was rejected in favour of a 2D measurement. In the 2D images all the shape information for assessment of shape energy of 3D larvae is stored. Viability tests are performed on 10 to 20 larvae in the veterinary practice, thus the implementation of a minimization process for the total energy is impossible because of the high probability of an overlap of larvae. The first term (bending) of F (Eq. (1)) contains the essential information for a viability classification (Alexander, 1986; Backholm et al., 2013). This term is calculated from the 2D contour, yielding in Eq. (2) (Fontoura Costa and Cesar, 2009; Ochoa et al, 2010; Vliet and Verbeek, 1993; Young et al., 1974):

$$F_{bending, image} = \frac{1}{P} \oint K^2 dS \qquad (2)$$

P − perimeter of contour K − local curvature dS − contour.

The total bending energy of a larvae group is obtained by the sum of all local curvature components in $F_{bending, image}$ (Eq. (2)). For the classification of the physiological state (Cangelosi and Meschke, 2014), statistical moments of the bending energy distributions are used. For a group, viability is assumed to be identical to its total bending energy except for a scaling quantity. In addition, the degree of spiralization of identified single larvae is determined by the VTD. Spiralization is correlated with the bending energy according to our investigations and used for energy control data.

3. Material and methods

3.1. Realisation of the VTD technique

The link between metabolism and form enables the design of a contactless and non-destructive measuring method of viability. This method is realized in the VTD, it is based on the optical recording of larvae contours by transmitted light in Near infrared wavelengths (Vogel and Venugopalan, 2003; Jacques, 2013). The wavelength range between 835 nm and 865 nm is used for forming an optimal contrast between the larvae and the surrounding medium (water-HCL-pepsin mixture, tissue). Another reason for selecting this narrow wavelength range is minimizing of errors in the identification of contours. The radiation path of the transmitted light through a larva near the edge depends on its radius. A decreasing radius shifts the identified edge from the real edge to the center line of the larva on the camera sensor. Since the optical depth (absorption and scattering) depends on the wavelength, minimization of the uncertainty in the edge detection is performed by using the narrow wavelength range (Zege et al., 1991; Van de Hulst, 1981). Additional, this means that the VTD is not susceptible to disturbing environmental light and presents no health risk to the staff. Circular or quadratic petri dishes are displayed on a quadratic video chip by

the optical system, with a minimum loss of information. Fig. 2 shows the VTD without workstation for use in the laboratory: the petri dish is placed in a mould in the window for the sample transfer. The calibration, device control, evaluation and reporting is all software-controlled and requires no intervention by the user. Raw data are stored together with temperature data from the surface of the liquid.

The key components of the VTD are a NIR-sensitive camera (UI-3770CP-NIR, IDS, Germany) equipped with a 1″ CMOS areal image sensor (CMV4000, CMOSIS, Belgium), a non-telecentric lens for 1″ sensors including bandpass filter, and a pulse-width modulated LED illumination system. High pixel pitch and a large geometric resolution, which are guaranteed by the camera, are of great importance for recognising nematode larvae contours. A color depth of 8 bits has proved to be sufficient. At the beginning and at the end of all captured image series, the surface temperature is measured contactless in the petri dish with the help of infrared radiation thermometers on the liquid surface (CSLT15, Optris, Germany), also using the emissivity of water for the HCI-pepsin solution. The camera and image acquisition, LED and temperature sensors, and evaluation are computer-processed.

Modules from the library of Heurisko image analysis software (AEON, 2017) are integrated in the software developed for the VTD.

Using the VTD, a header including camera and illumination processing data, temperature data and all the raw 2D images of a series are packed into a single 3D (2½D) raw data block for evaluation and documentation.
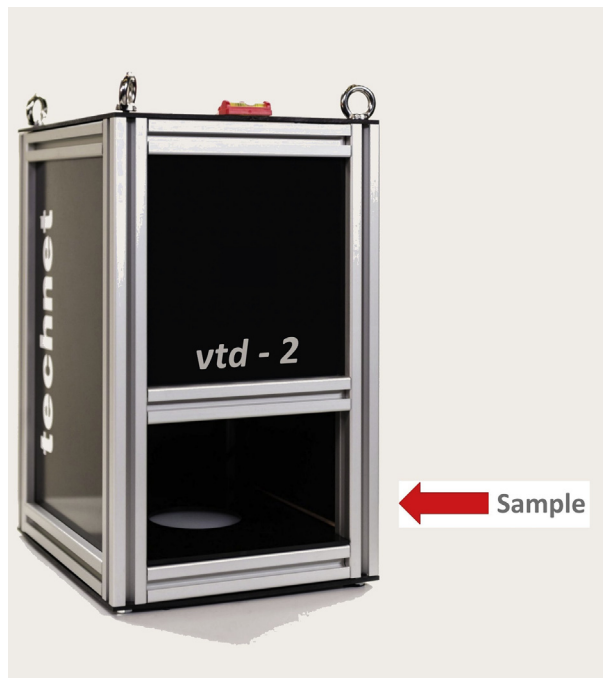

Fig. 2. Viability Test Device (length × width × height: 300 mm × 250 mm × 500 mm).

The VTD has four different modes of investigation, depending on the different workflows in a lab:

- Calibration data acquisition

- Data acquisition and subsequent evaluation

- Data acquisition without subsequent evaluation

- Data analysis without data acquisition

The results, including details from the client, laboratory and samples, are logged in a protocol.

To unlock the VTD system, reference images are generated as a first step by empty petri dishes of the same batch. Images for viability test series are calibrated by radiometric two-point calibration (Jähne, 2012a) based on the generated reference images.

For a rapid check of the operating of the VTD, ETFE (Ethylene tetrafluoroethylene) films (thickness 250 μm) printed with standard patterns (Maywald and Riesser, 2016) are positioned in petri dishes. In the wavelength range used by VTD, the films are 95% translucent, the different printed areas reflect light from 100% to 50%. By help of these patterns, artificial curvature data and viability states are simulated. Deviations from known target data enable fast detection of system faults (electronic drifting of the camera electronics, radiation behavior of the NIR-LEDs, numerical evaluation problems, …). Fig. 3 shows control patterns with different NIR light transmission of the printing areas (0% left, 50% right).

No thermal corrections or extensions for the different viscosity of the surrounding medium were undertaken in these studies, since all of the experiments were carried out in identical solutions within the range 19.5°−21.5 °C.
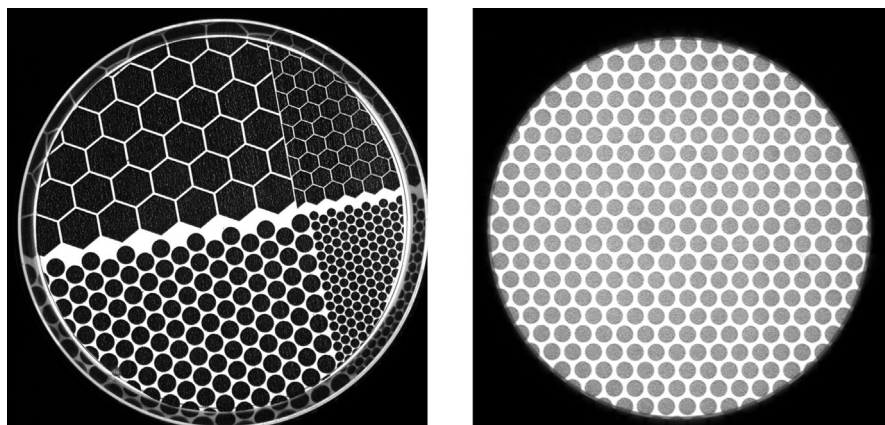

Fig. 3. Test pattern for system control: IR-transmissivity of dark areas (0%, left), (50%, right).

3.2. Biological test material

Measurements of anisakid larvae were conducted on *Anisakis simplex s.s.* from herring. The anisakid larvae were identified following the morphological criteria proposed by Berland (2003).

Live larvae (n = 400) were isolated from fresh herring intestines by digestion using a pepsin/HCL-solution according to Karl et al. (2014), visually checked for mobility and kept in 0.9 % NaCl-solution at 4 °C until applied to the VTD on the same day.

Deep-frozen larvae (n = 100) were prepared by freezing fresh isolated larvae in tap water in a test tube at −20 °C for at least two days.

Salted dead nematode larvae (n = 80) were isolated from salted herring. To prepare salted herring, 2.5 kg of fresh whole herring (without gills) and 425 g of salt were mixed manually in a plastic box, the closed box stored for 12 h at 3 °C and the herring covered with 20 % salt brine (w/w). To avoid a salt gradient, the box was shaken carefully several times during cold storage. After 4 month of storage, nematode larvae were isolated from the salt cured herring intestines by pepsin/HCL and stored in 20% NaCl-solution.

Dead nematodes from marinated herring fillets were prepared by placing live nematode larvae on the flesh side of a herring fillet which was covered with a second fillet. The fillets were fixed by means of a small rubber band. 1.5 kg of freshly prepared double fillets of herring were placed in a plastic box and covered with 1 L of marinating brine (6 % vinegar/13 % salt). The box was closed and stored, with repeated careful shaking, for 48 days at 2 °C. A total of 90 nematode larvae were isolated from the marinated herring fillets by pepsin/HCL and stored in 0.9 % NaCl-solution.

Staining procedure

The staining procedure followed the methods of Leinemann and Karl (1988). Nematode larvae were placed for 24 h at 33−35 °C in a staining solution and visually inspected for staining. The staining bath consisted of 90 ml pepsin/HCL-solution mixed with 10 ml fuchsine solution (1 % w/w in water). Dead nematodes will be stained, whereas live nematodes remain uncoloured.

Pepsin/HCL solution

50 g pepsin (2000 FIP/g) and 54 ml HCL 37 % are dissolved in 10 L tap water.

VTD readings

The number of nematodes used for a single VTD reading ranged from 1 to 20 individuals. Details are found in the respective chapters. Each reading consisted of maximal 50 images.

Comparison of VTD results and staining procedure

Larvae, inactivated by deep freezing, marinating or salting, and live larvae were isolated, transferred to a petri dish filled with a small layer of pepsin/HCL solution and examined by the VTD. Afterwards the larvae were placed immediately in 20 ml fuchsine staining solution and kept at 33 °C for 24 h. The tests were repeated several times.

All examinations were conducted at an almost constant environmental temperature of 20 °C in a liquid medium (water, pepsin, HCl).

3.3. Software development and application

For numerical handling the discretised model larva is separated into a topological, a geometric and a physical part. The topological part describes the connection between the discrete points, the geometric part provides coordinates of all points. The physical part is used to describe the interaction of the points among each other and under external influences (Gründig, 1985; Ströbel et al., 2016). The individual parts are allocated to matrices, which enable the reproduction of the measured contours by a form-finding process for the assigned minimum energy shapes (Schmidt, 2007) and consequently to the viability.

To visualise the working method of the VTD, the 3D shape of the larvae is created from the measured 2D contour data, assuming a circular cross-section (Fig. 4a left). At each discrete point on the surface, normal vectors and muscle tensions are calculated. Local curvatures of all surface positions are determined from neighbouring normal vectors by these means. In operation the VTD determines the normal vectors for 2D contours (Nordberg et al., 1995) and determines the associated elastic curvature energies (Fig. 4b right). Constant material
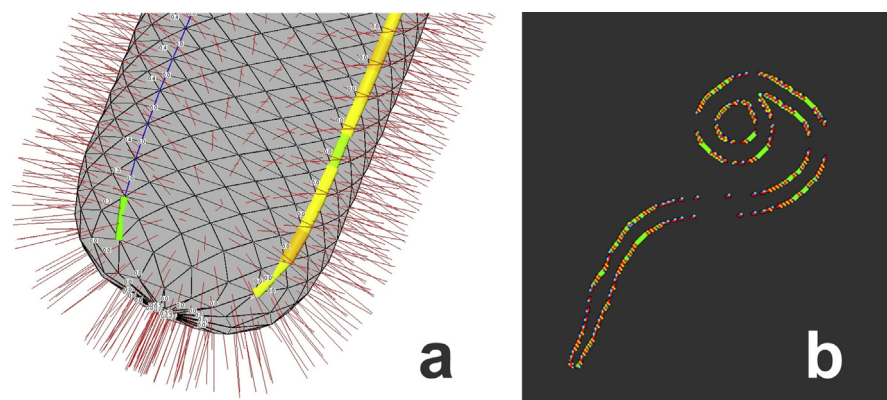

Fig. 4. Visualisation of normal vectors on the surface of a 3D larva model with colour-coded muscle tension (a), colour-coded bending energies in the 2D contour image (b).

characteristics are used for the interaction between neighbouring points. The determination of viability is thus limited to the direct study of curvature characteristics of contours.

By examining individual objects, the numeric process described provides important indications for understanding the shape of larvae. Since ensembles of larvae are usually examined in laboratory practice there is a high probability of aggregation and overlapping of object contours (Fig. 1) (Yang et al., 2010). The mobility manifests in a variation of topological characteristics of surface patterns within an image series (Barth et al., 2001). Therefore, the VTD determines viability for a larvae ensemble from statistical distributions of local curvature parameters, ignoring quantities caused by surface stress and inner pressure. Additional, for all identified objects the degrees of spiralization are determined. The interval of degree of spiralization without turns s ranges from straight (s = 0) to circle (s = 1). Experiments have shown that a limited number of 20 objects in a petri dish requires no weighting of the statistical distributions of bending energy and spiralization.

In order to take into account large and small curvatures with their different significance for viability determination (Weerasooriya et al., 1986; Tejada et al., 2006), the described curvature and spiralization distributions are conducted by a multigrid representation in a multiscale space (Jähne, 2012b; Mokhtarian and Mackworth, 1992). A matrix is generated from each individual image in a series, which contains the normed histogram data for different geometric scales (fine to coarse resolutions). These input matrices enables to revert to the methods of spectrum interpretation that are customary in the field of chemistry (Günzler and Gremlich, 2002; Manley, 2014). Studies on the time-dependency of larva shapes were evaluated by means of Partial Least Square Regression (PLSR). To this end, the datasets were split randomly into a calibration part for regression analysis and a validation part for the purpose of control (Daschner, 2002; Kent, 2005).

To associate different larvae shapes with production processes (e.g. deep freezing, salting, marinating), scale-dependent feature vectors are extracted from the distribution matrices. By minimum-distance-clustering technique (Celenk, 1990; Haberäcker, 1995) viability factors are calculated from the feature vectors.

The output log of the VTD is shown in Fig. 5. It summarises all of the relevant information on a conducted viability determination to laboratory standards. The measurement data used are the maximum and mean viability factors, including standard deviation, the proportion of living and dead objects, and the temperature of the medium in the petri dish for an individual sample.

VTD – Report
Viability Test Device

Project data		Sample	
Date:	28.10.2016	Receipt date:	20.01.2016
Time:	11:04:17	Receipt time:	14:30
Host species:	Clupea harengus	Receipt packaging state:	3
Parasite species:	Anisakis simplex	Receipt temperature:	2.3
Product:	Frozen	Client code:	MRI-20
Number of images:	50	Client charge:	3
Measuring interval:	1	Storage temperature:	-12.5
Number:	001	Locality of storage:	Hamburg
Dataset:	Parasite-001	Sample receipt person:	R.Gleisinger

Client		Contractor	
Company/Lab:	Nemalab		technet Gmbh
Division:	Seafood		Membrane technology
Contact person:	Dr.C.Herrmann		M.Kroeger
Street/Postbox	Nemaweg 12		Pestalozzistraße 8
Zip code:	D-63452		D-70563
City:	Hanau		Stuttgart
Fon:	+49 123456		+49 711 12345
Fax:	+49 654321		+49 711 54321
Email:	info@nemalab.com		michael.kroeger@technet-gmbh.com
URL:	www.nemalab.com		www.technet-gmbh.com

Results	
Maximal viability factor:	0.9
Mean viability factor:	0.84
SD viability factor:	0.08
Objects alive (%):	98
Objects dead (%):	2
Temperature (°C):	22.3

Fig. 5. Output log of the VTD for a single sample (image series).

4. Results and discussion

4.1. Significance of the curvature distribution and spiralization for determining viability

4.1.1. Studies of individual animals

One test of the model formation implemented in the VTD is the comparison of larvae of an (almost) equal and constant state of viability. To this end, 5 individual *Anisakis*

larvae were isolated from the intestines of a freshly-caught herring (*Clupea harengus*) and immediately examined. It was assumed of these larvae that they had a similar and maximum viability. 250 contour images were taken from each larva at a time interval of 12.5 msec (Fig. 6).

Fig. 7 shows the similarities of the spiralization (light blue) and bending energies (dark blue) related to each mean value (100%) for the 250 camera shots of the 5 objects studied.

4.1.2. Long-term studies

In a long-term study it was tested whether the measured curvature parameters (bending energy and spiralization) are suitable for illustrating the physical or biological reality when objects in a state of high viability pass into a state of low viability. To this end, an ensemble of 10 nematode larvae (*Anisakis simplex*, herring) was observed using the VTD in a long-term experiment without energy supply (nutrition) in a liquid without CO_2 management (water, pepsin, HCl) (Dàvila et al., 2006) in the time frame that is relevant to seafood production, namely 30 days. In total, 800 individual images were generated without changing the experimental configuration. The objective was to prove the changes in viability with the described curvature analysis. To this end, the distribution patterns of the bending energy and of spiralization on 4 scales were combined. Fig. 8 shows the decreasing mean bending energies and mean degrees of spiralization of the larvae ensemble within a period of 30 days.

The measured data are attributed to different curvature phases of the larvae: varying spiralization changes into a strong stable formation, followed by relaxation (Isele-Holder et al., 2015). For the long-term study the turning point was identified by VTD from the change of curvature diversity. For each series the kurtosis of the distributions of bending energy and spiralization were calculated as a measure of their structure diversity (Leach, 2001). The temporal development of the kurtosis has a
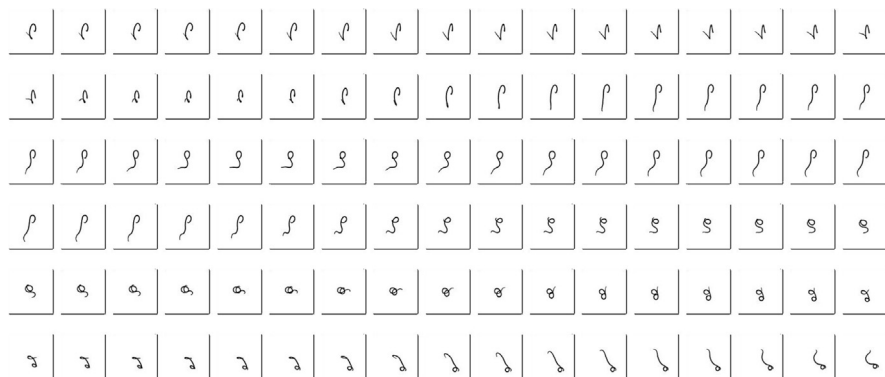

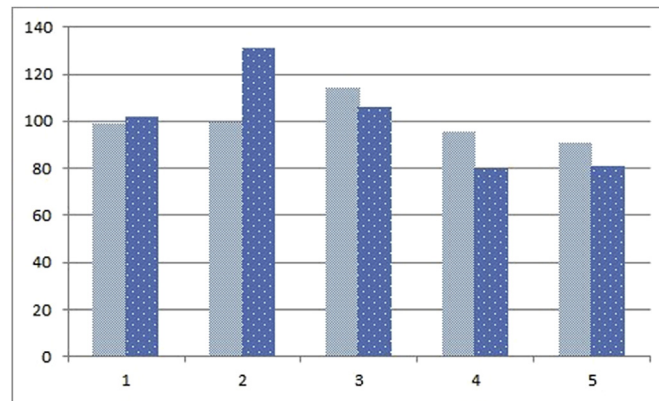**Fig. 6.** Excerpt of a recorded sequence of larvae at intervals of 12.5 msec.

Fig. 7. Distribution around the mean value (100%) of the degree of spiralization (light) and the bending energies (dark).
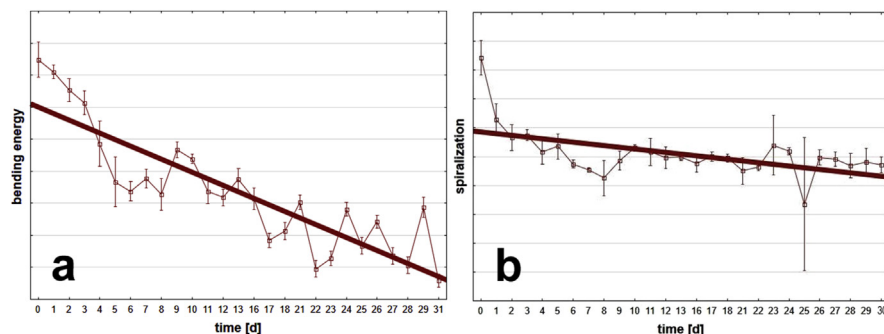

Fig. 8. Decreasing of bending energy (a) and spiralisation (b) for an ensemble within the first 30 days.

minimum approximately on day 10 for the measured data (Fig. 9) in accordance with visual observations. The minimum state values can be used for thresholding (viable/ not viable).

In the diagrams the relative factors for viability are shown without units.

After 30 days, the visual observation of the nematode larvae (CODEX STAN 244, 2004) showed no further movement. The VTD data, however, still displayed a low level of remaining activity after this period. The viability state is determined by the VTD with a high level of precision, which cannot be achieved with simple optical systems.

To prove the quality of the applied model all the spiralization and curvature matrices for all scales were examined by the Partial Least Square Regression method (PLSR). Histogram data from bending energy and spiralization distributions for different scales are used as input variables. Results confirmed the correct description of time dependent shift of viability by spiralization and bending energy distribution (Fig. 10).
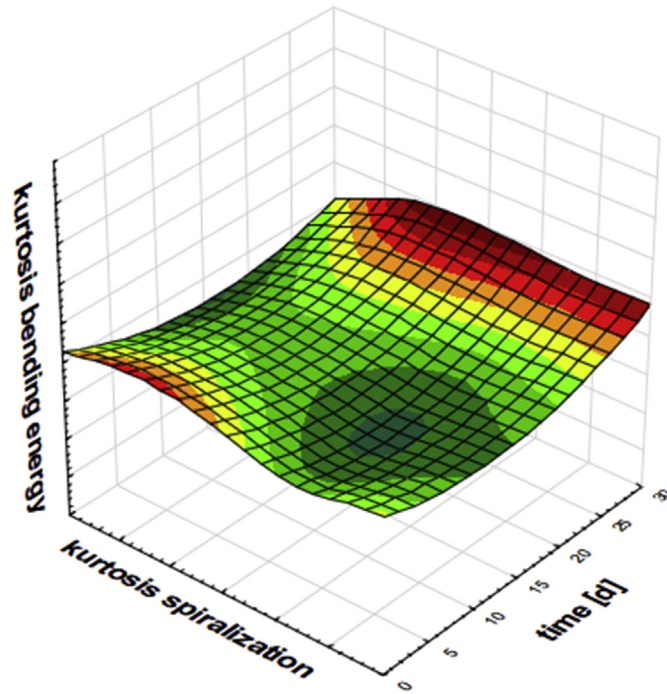
Fig. 9. Temporal variation of kurtosis of degrees of spiralization and bending energy for an ensemble within the first 30 days.

4.2. Product examinations

The objective of the VTD development is to provide a system for the safe and fast risk assessment of infection from living anisakids in the manufacture of seafood products. To check the viability in fish fillet, three steps are necessary. In a first
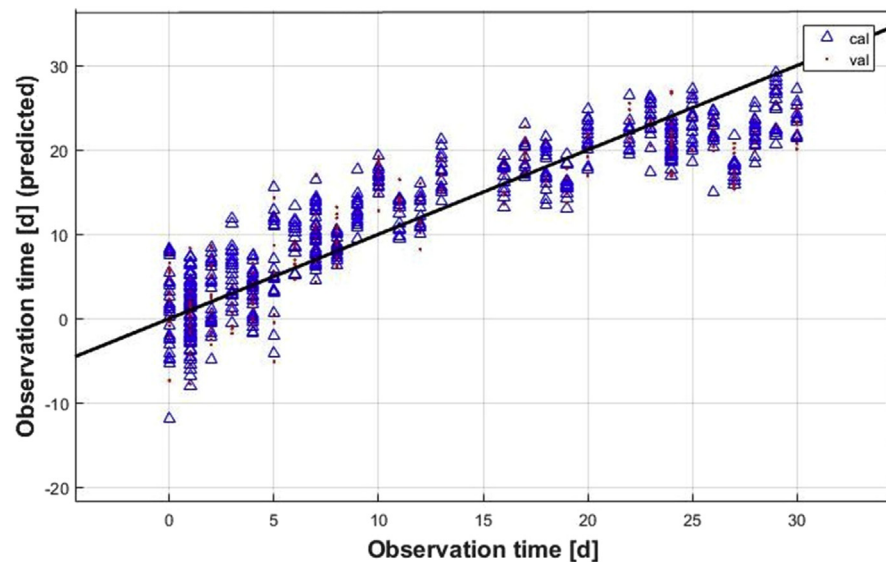

Fig. 10. Calculation of the coefficient of determination for the first 30 [d]. Coefficient of Determination R^2: 0.821 Root Mean Square Error for Calibration/Validation $RMSE_{cal/val}$: 4.10/4.37.

step, the larvae have to be isolated by the digestion method, which takes about 2 hours. To avoid possible underestimation of embedded larvae (Gómez-Morales et al., 2017) the digestions conditions as described by Karl et al. (2014) should to be followed strictly. The isolated larvae are transferred to a petri dish filled with a small layer of pepsin/HCL solution and the petri dish is placed in the VTD. The repeated measurement and readout by the VTD takes only few minutes (Fig. 11).

The reliability of the purely geometric approach for calculating viability from combined bending energy and spiralization distributions was proven in the long-term study. Another test of the system was conducted by measuring the influence of the production process on the shape energy distribution patterns of anisakids. To this end, in line with production methods customary for Germany, hard-salted and marinated herring products were manufactured, from which inactivated nematode larvae were isolated. Furthermore, living larvae were deep-frozen in water at −20 °C. In several experiments, series of 50 images each were generated of living larvae (100 series), deep-frozen larvae (60 series), from salted (80 series) and marinated (90 series) products. The image series were examined in accordance with a secure separation of living from dead larvae. A warning of a possible risk of viability (infection) is issued by the VTD when threshold (0.70) is exceeded, however the threshold can be adjusted by authorised users. In order to be able to take account of mixtures of individual objects with very different viability factors, the standard deviation, the maximum viability factor of the individual objects, and the proportion
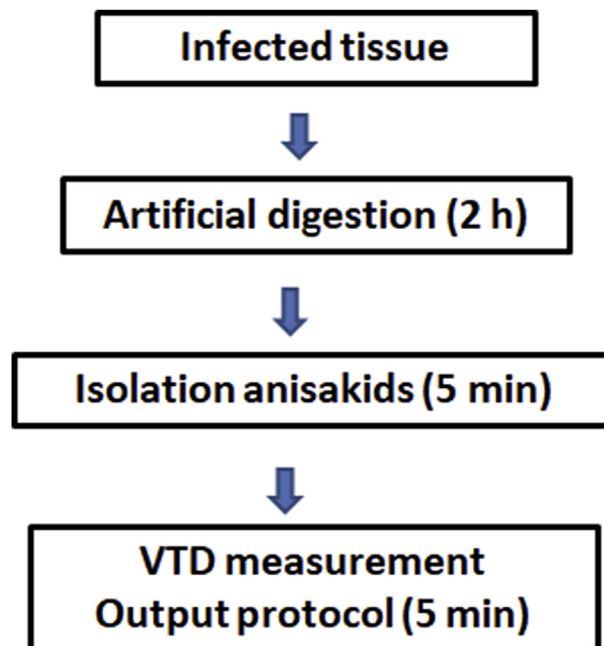

Fig. 11. Process flow of the VTD viability test procedure.

of objects with a viability factor above and below the set threshold are also issued in addition to the mean value (living/dead [%]).

The production process also has an influence on the local curvature characteristics of larvae. In Fig. 12 shows the strong dependency of the mean viability factors on the production process. The reasons for this are by and large unexplained and require further examination.

In comparative analyse of 50, 25, 10 and 5 images/series, evaluations for 20 images/series, generated at a time interval of 500 msec, have proven to be the best compromise for exactness, speed and storage requirements. However, series of 50 images are implemented as default detection variables in the VTD. Experts can use these series as short movies to complement the usual visual examination of mobility. For the described evaluation, however, only every second image of a series is used (default). The data recording of a single sample (petri dish) takes 30 sec, while evaluation and reporting take a further 60 sec.

From the ratio between the viability factors of the product tissue to the viability factor of raw tissue, the inactivation rate of a process as a measure of safety of the seafood product can be calculated (Eq. (3)):

$$Inactivation\ rate = Viability\ factor_{product\ tissue} \big/ Viability\ factor_{raw\ tissue} \tag{3}$$

4.3. Comparison of VTD results with visual inspection and staining

To verify the results obtained from the test device for deep frozen and salt-inactivated larvae, the staining test was applied on randomly taken same mixtures of dead and live nematode larvae after a readout by the VTD. After staining, the
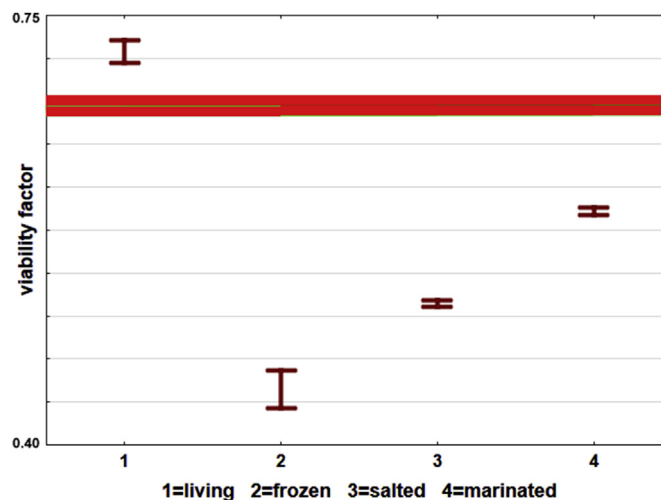

Fig. 12. Viability factors for different production processes (97 series, 4,850 images).

larvae were additionally inspected visually for movement. The staining method based on the fact that the death of nematodes results in an increased cuticle permeability and the stains colour the whole nematodes, whereas live larvae remain unstained. The limitation of this procedure is the occurrence of semi-coloured nematodes (Leinemann and Karl, 1988; Vidacek et al., 2010).

4.3.1. Differentiation of live and deep frozen larvae

Table 1 shows the results for two test mixtures of deep frozen and live nematode larvae. Virtually all initially live nematodes remained uncoloured and showed either slight or strong motion. But only parts of the 20 dead nematodes were completely coloured, 12 were only partially stained. None of these nematodes showed active movements. The VTD readout reflects the initial number of dead and live nematode larvae.

4.3.2. Differentiation of live and salt-inactivated nematode larvae

The results of two tests with salt-inactivated nematodes are compiled in Table 2.

In the first experiment (Test no. 3.9) only dead nematodes were examined. The staining test and visual inspection showed that all were at least half stained and motionless.

The VTD readout was 97.1 % dead and 2.9% live. These values refer to the viability of the whole ensembles and are obtained by applying the threshold to the entire curvature distribution. Experts, in contrast, decide for individual objects by estimating each state of motion. In considering the slow transition from life to death, the VTD delivers non-integer values, while the visual estimates by experts always produce integer values. Even when the VTD results are rounded there are minor deviations from the data that were obtained under visual inspection.

In the second experiment (Test no. 3.10), 5 live and 20 salt-inactivated NL were mixed and examined. Three live larvae remained uncoloured, but two were little coloured whereas the dead larvae were either partially or completely coloured. Again the VTD results reflect the initially mixed number of dead and live larvae.

Table 1. Staining test, visual inspection and VTD results of deep frozen versus live nematodes.

Test no	Nematode mixture No/%		Degree of coloration and motion by naked eye (experts), No/%			VTD	
	Live	Dead	Uncoloured	Partially coloured	Coloured	Live [%]	Dead [%]
2.6	5/33	10/66	6/40[a]	3/20[c]	6/40[c]	34.8	65.2
2.8	4/28	10/71	4/27[b]	9/60[c]	1/7[c]	28.8	71.2

a = slight motion, b = active, c = motionless.

Table 2. Staining test, visual inspection and VTD results of salted versus live nematodes.

Test no	Nematode mixture No/%		Degree of coloration and motion by naked eye (experts), No/%			VTD	
	Live	Dead	Uncoloured	Partially coloured	Coloured	Live [%]	Dead [%]
3.9	0/0	10/100	0/0	3/30[c]	7/70[c]	2.9	97.1
3.10	5/20	20/80	3/12[b]	7/28[c] 2/8[a]	13/52[c]	22.5	77.5

a = slight motion, b = active, c = motionless.

The experiments showed that the VTD readout was able to detect the initial number of mixed dead and live nematode larvae, whereas the staining always yielded partly-coloured larvae, which are difficult to assign to dead or live nematodes.

5. Conclusion

Increasing demands on the quality of seafood products and the guarantee of their health safety requires monitoring methods that allow a simple and low cost control (Kroeger, 2009). The VTD allows automated optical inspections independent of visual observations of experts, by reading and analysis the elastic shape parameters from contour images. Our studies of mobility of larvae in the context of food safety controls showed that elastic form energies reflect their metabolic activity. For the sake of simple handling, no multispectral and 3D information is obtained. Calibrated image series are used to calculate geometric curvature characteristics, whose correlation with data from the visual inspection has proven to be valid in experiments. Studies with individual larvae and groups of larvae have shown that the VTD illustrates the biological processes realistically with regard to their viability. The device therefore allows the monitoring of production methods and production process in the seafood sector, independent of visual observation, and provides graduated results with defined permissible limits. Particularly this information, including raw data and reports, can be an important tool for the documentation (ISO 9000, 2008) of manufacturing processes and new developments (Oh et al., 2014).

Declarations

Author contribution statement

Michael Kroeger: Conceived and designed the experiments; Performed the experiments; Analyzed and interpreted the data; Contributed reagents, materials, analysis tools or data; Wrote the paper.

Competing interest statement

The authors declare no conflict of interest.

Additional information

No additional information is available for this paper.

References

AEON, 2017. http://www.aeon.de/en/heurisko_products.html. (Accessed 15 August 2017).

Alexander, R.McN., 1986. Bending of cylindrical animals with helical fibres in their skin or cuticle. J. Theor. Biol. 124 (1), 97−110.

Backholm, M., Ryu, W.S., Dalnoki-Veress, K., 2013. Viscoelastic properties of the nematode *Caenorhabditis elegans*, a self-similar, shear-thinning worm. Proc. Natl. Acad. Sci. Unit. States Am. 110, 4528−4533.

Barth, E., Ferraro, M., Zetzsche, C., 2001. Global topological properties of images derived from local curvature features. Notes in Computer Science, pp. 285−294.

Berland, B., 2003. *Anisakis* spp. In: Akuffo, H., Linder, E., Ljungström, I., Wahlgreen, M. (Eds.), Parasites of the Colder Climates. Taylor & Francis, Abingdon, pp. 161−168.

Biedermann, I., 1985. Human image understanding: recent research and theory. Comput. Vis. Graph Image Process 32, 29−73.

Butler, M., Spearman, M., Braasch, K., 2014. In: Pförtner, R. (Ed.), Animal Cell Biotechnology, Methods in Molecular Biology, vol. 1104, pp. 169−192.

Cangelosi, G.A., Meschke, J.S., 2014. Dead or alive: molecular assessment of microbial viability. Appl. Environ. Microbiol. 80 (19), 5884−5891.

Celenk, M., 1990. A color clustering technique for image segmentation. Comput. Vis. Graph Image Process 52, 145−170.

Clark, R.B., Cowey, J.B., 1958. Factors controlling the change of shape of cetain nemertean and turbellarian worms. J. Exp. Biol. 35, 731−748.

CODEX STAN, 2004. Standard for Salted Atlantic Herring and Salted Sprat, Annex I. Joint FAO/WHO Food Standards Programme, 244.

Daschner, F., 2002. Multivariate Messdatenverarbeitung für die dielektrische Spektroskopie mit Mikrowellen zur Bestimmung der Zusammensetzung von Lebensmittel. Shaker Verlag, Aachen.

Davey, H.M., 2011. Life, death, and in-between: meanings and methods in microbiology. Appl. Environ. Microbiol. 77 (16), 5571−5576.

Dàvila, C., Malagón, D., Valero, A., Benitez, R., Adroher, F.J., 2006. *Anisakis simplex*; CO_2-fixing enzymes and development throughout the in vitro cultivation from third larval stage to adult. Experimental Prasitology 114 (1), 10−15.

Deserno, M., 2014. Fluid lipid membranes: from differential geometry to curvatures stresses. Chem. Phys. Lipids 185, 11−45.

Fontoura Costa, L., Cesar Jr., R.M., 2009. Shape Characterization. In: Costa, Fontoura, Cesar (Eds.), Shape Classification and Analysis. CRC Press, Boca Raton, pp. 403−447.

Giese, M.H., Poggio, T., 2003. Neural mechanism for the recognition of biological movements. Nat. Rev. Neurosci. 4 (3), 179−192.

Giarratana, F., Giuffrida, A., Gallo, F., Ziino, G., Panebianco, A., 2012. Study on the resistance variability of *Anisakis* larvae to some technological stressors. In: Pugliese, A., Gaiti, A., Boiti, C. (Eds.), Veterinary Science. Springer-Verlag, Berlin Heidelberg, pp. 155−159.

Giarratana, F., Muscolino, D., Ziino, G., Giuffrida, A., Marotta, S.M., Presti, V.L., Chiofalo, V., Panebianco, A., 2017. Activity of *Tagetes minuta* Linnaeus (Asteraceae) essential oil against L3 *Anisakis* larvae type 1. Asian Pac. J. Trop. Med. 10 (5), 461−465.

Gómez-Morales, M.A., Martínez Castro, C., Lalle, M., Fernández, R., Pezzotti, P., Abollo, E., Pozio, E., The Ring Trial and -testing Participants, 2017. UV-press Method Versus Artificial Digestion Method to Detect Anisakidae L3 in Fish Fillets: Comparative Study and Suitability for the Industry. Fisheries Research in Press.

Goriely, A., Tabor, M., 2013. Rotation, Inversion, and Perversion in Anisotropic Elastic Cylindrical Tubes and Membranes. OCCAM, Mathematical Institute, University of Oxford.

Grabda, J., 1991. Marine Fish Parasitology: an Outline. Wiley-VCH, Weinheim.

Günzler, H., Gremlich, H.-U., 2002. Quantitative spectroscopy. In: IR Spectroscopy. Wiley-VCH, Weinheim.

Gründig, L., 1985. The force-density-approach and numerical methods for the calculation of networks. In: Proceedings 3. International Symposium Wide Span Surface Structures, pp. 99−106. Stuttgart, Germany.

Haberäcker, P., 1995. Minimum-distance-cluster-algorithmus. In: Praxis der Digitalen Bildverarbeitung und Mustererkennung. Carl Hanser Verlag, München.

Harris, J.E., Crofton, H.D., 1957. Structure and function in the nematodes: internal pressure and cuticular structure in ascaris. J. Exp. Biol. 34, 116−130.

Helfrich, W., 1973. Elastic properties of lipid bilayers: theory and possible experiments. Z. Naturforsch. C Biosci. 28, 693−703.

Hirasa, K., Takemasa, M., 1998. Spice Science and Technology. CRC Press, Boca Raton.

Isele-Holder, R.E., Elgeti, J., Gompper, G., 2015. Self-propelled worm-like filaments: spontaneous spiral formation, structure, and dynamics. Soft Matter 11, 7181−7190.

ISO 9000, 2008. Document: ISO/TC 176/SC 2/N525R2, ISO 9000 Introduction and Support Package: Guidance on the Documentation Requirements of ISO 9001:2008.

Jacques, S.L., 2013. Optical properties of biological tissues: a review. Phys. Med. Biol. 58, R37−R61.

Jähne, B., 2012a. Inhomogeneous point operations. In: Jähne (Ed.), Digital Image Processing. Springer-Verlag, Berlin, pp. 234−241.

Jähne, B., 2012b. Multiscale representation. In: Jähne (Ed.), Digital Image Processing. Springer-Verlag, Berlin, pp. 121−138.

Karl, H., Ostermeyer, U., Bauer, H., Miller, A., Mohn, K., Müller-Hohe, E., Neuhaus, H., Pölzelbauer, C., Stumme, B., Walter, M., Wernusch, J., Werth, B.-M., Wittmann, C., 2014. Collaborative Study for Quantification of Anisakis Larvae in Spiked salmon Fillets (Salmo salar) by a Modified Codex Digestion Method. J. Verbr. Lebensm. 9 (4), 359−365.

Kent, M., 2005. Multivariate analysis. In: Kent, M., Knöchel, R., Barr, U.-K., Tejada, M., Nunes, L., Oehlenschläger, J. (Eds.), SEQUID − A New Method for Measurement of the Quality of Seafood. Shaker Verlag, Aachen.

Khairy, K., Howard, J., 2011. Minimum-energy vesicle and cell shapes calculated using spherical harmonics parameterization. Soft Matter 7, 2138−2143.

Kroeger, M., 2009. Image processing. In: Rehbein, H., Oehlenschläger, J. (Eds.), Fishery Products- Quality, Safety and Authenticity. Wiley-Blackwell, Chichester, pp. 240−251.

Leach, A.R., 2001. The use of molecular modelling and chemoinformatics to discover and design new molecules. In: Leach (Ed.), Molecular Modelling. Pearson Educationl Limited, Harlow, pp. 640−719.

Leibler, S., 2004. Equilibrium statistical mechanics of fluctuating films and membranes. In: Nelson, D., Piran, T., Weinberg, S. (Eds.), Statistical Mechanics of Membranes and Surfaces. World Scientific, New Jersey, pp. 49−101.

Leinemann, M., Karl, H., 1988. Untersuchungen zur Differenzierung lebender und toter Nematodenlarven (*Anisakis sp.*) in Heringen und Heringserzeugnissen. Arch. Leb. 39, 147−150.

Levsen, A., Lunestad, B.T., 2010. Anisakis simplex third stage larvae in Norwegean spring spawning herring (*Clupea harengus* L.), with emphasis on larval distribution in the flesh. Vet. Parasitol. 171 (3-4), 247−253.

Llanera-Reino, M., Pineiro, C., Antonio, J., Outerino, L., Vello, C., Gonzales, A.F., Pascual, S., 2013. Optimization of the pepsin digestion method for anisakids inspection in the fishing industry. Vet. Parasitol. 191, 276−283.

Lucius, R., Loos-Frank, B., 2008. Nematoda. In: Biologie von Parasiten. Springer, Berlin, pp. 367−402.

Manley, M., 2014. Near-infrared spectroscopy and hyperspectral imaging: non destructive analysis of biological materials. J. Chem. Soc. Rev. 43, 8200−8214.

Maywald, C., Riesser, F., 2016. Sustainability − the art of modern architecture. Procedia Eng. 155, 238−248.

Mattiucci, S., Nascetti, G., 2008. Advances and trends in the molecular systematics of anisakid nematodes, with implication for their evolutionary ecology and host-parasites co-evolutionary processes. Adv. Parasitol. 66, 47−148.

Maturin, L., Peeler, J.T., 2001. Aerobic plate count. In: Food and Drug Administration (FDA), Bacteriological Analytical Manual. https://www.fda.gov/food/

foodscienceresearch/laboratorymethods/ucm063346.htm. (Accessed 15 August 2017).

Milligan, R.J., 2008. The Occurrence and Behaviour of Pseudoterranova dcipiens and Anisakis simplex (Nematoda) in Gadus morhua and their Impacts on Commercial Processing. MSc(R) thesis. University of Glasgow. http://theses.gla.ac.uk/252/. (Accessed 22 August 2017).

Mokhtarian, F., Mackworth, A.K., 1992. A theory of multiscale, curvature-based shape representation for planar curves. IEEE Trans. Pattern Anal. Mach. Intell. 14 (8), 789−805.

Moon, S., Lee, S., Kim, H., Freitas-Junior, L.H., Kang, M., Ayong, L., Hansen, M.A.E., 2013. An image analysis algorithm for malaria stage classification and viability quantification. PLoS One 8 (4), e61812.

Nieuwenhuizen, N.E., Lopata, A.L., 2013. Anisakis − A food-borne parasite that triggers allergic host defences. Int. J. Parasitol. 43, 1047−1057.

Nordberg, K., Knutsson, H., Granlund, G., 1995. Local Curvature from Gradients of the Orientation Tensor Field. Computer Vision Laboratory, Linköping University. LiTH-ISY-R-1783.

Ochoa, D., Gautama, S., Philips, W., 2010. Automatic identification of *Caenorhabditis elegans* in population images by shape energy features. J. Microsc. 238, 173−184.

Oh, S.-R., Zhang, C.-Y., Tea-Im, K., Sung-Jong, H., In-Sun, J., Sun-Ho, L., Soon-Han, K., Joon-Il, C., Sang-Do, H., 2014. Inactivation of *Anisakis* larvae in salt-fermented squid and pollock tripe by freezing, salting, and combined treatment with chlorine and ultrasound. Food Contr. 40, 46−49.

Pascual, S., Antonio, J., Cabo, M.L., Pineiro, C., 2010. Anisakis survival in refrigerated fish products under CO_2 modified-atmosphere. Food Contr. 21, 1254−1256.

Posset, T., Gaus, H., Dearden, M., Becker, M., Eicher, R., 2017. Visual Inspection of Medicinal Products for Parenteral Use. ECA Academy. www.visual-inspection.org. (Accessed 16 August 2017).

Priebe, K., Jendrusch, H., Haustedt, U., 1973. Problematik und Experimentaluntersuchungen zum Erlöschen der Einbohrpotenz von Anisakis-Larven des Herings bei der Herstellung von Kaltmarinaden. Arch. Leb. 24 (9), 217−222.

Schmidt, B., 2007. Minimal energy configurations of strained multi-layers. Calc. Var. Partial Differ. Equ. 30 (4), 477−497.

Schrödinger, E., 1944. Order, disorder and entropy. In: What Is Life. Cambridge University Press, Cambridge, pp. 67−75 (2013 reprint).

Sommerfeld, A., 1950. Dynamics of deformable bodies. In: Mechanics of Deformable Bodies: Lectures in Theoretical Physics, vol. 2. Academic Press, New York, pp. 83−128.

Ströbel, D., Singer, P., Holl, J., 2016. Analytical form finding. Int. J. Space Struct. 31 (1), 52−61.

Sutton, S., 2011. Accuracy of plate counts. J. Validation Technol. 17 (3c), 42−46.

Svetina, S., Kuzman, D., Waugh, R.E., Ziherl, P., Zeks, B., 2004. The cooperative role of membrane skeleton and bilayer in the mechanical behavior of red blood cells. Bioelectrochemistry 62, 107−113.

Tejada, M., Solas, M.T., Navas, A., Mendizabal, A., 2006. Scanning electron microscopy of Anisakis larvae following different treatments. J. Food Protect. 69 (6), 1379−1387.

Van de Hulst, H.C., 1981. Circular cylinders. In: Light Scattering by Small Particles. Dover Publications, New York, pp. 297−328.

Vidacek, S., de las Heras, C., Solas, M.T., Mendizabal, A., Rodriguez-Mahillo, A.I., Tejada, M., 2010. Antigenicity and viability of *Anisakis* larvae infesting hake heated at different time-temperature conditions. J. Food Protect. 73 (1), 62−68.

Vliet, L.J., Verbeek, P.W., 1993. Curvature and bending energy in digitized 2D and 3D images. In: SCIA '93, Proceedings 8th Scandinavian Conference on Image Analysis (pp. 1403−1410), Tromsoe, Norway.

Vogel, A., Venugopalan, V., 2003. Mechanisms of pulsed laser ablation of biological tissues. Chem. Rev. 103 (2), 577−644.

Weerasooriya, M.V., Fujino, T., Yoichi, I., 1986. The value of external morphology in the identification of larval anisakid nematodes: a scanning electron microscope study. Z. für Parasitenkd. 72, 765−778.

Wertheimer, M., 1912. Experimentelle Studien über das Sehen von Bewegung. Z. für Psychol. und Physiol. Sinnesorgane 61 (1), 161−237.

Yang, Y., Marceau, V., Gompper, G., 2010. Swarm behavior of self-propelled rods and swimming flagella. Phys. Rev. E 82, 1−13, 031904.

Young, I.T., Walker, J.E., Bowie, J.E., 1974. An analysis technique for biological shape. Inf. Contr. 25, 357−370.

Zege, E.P., Ivanov, A.P., Katsev, I.L., 1991. Light scattering in semi-infinite media and plane layers illuminated by infinitely extented plane sources. In: Zege, Ivanov, Katsev (Eds.), Image Transfer through a Scattering Medium. Springer-Verlag, Berlin, pp. 26−64.

Zheng, W., Liu, J., 1993. Helfrich shape equation for axisymmetric vesicles as a first integral. Phys. Rev. 48 (4), 2856−2860.

Zhong-can, O., Helfrich, W., 1989. Bending energy of vesicle membranes: general expressions for the first, second, and third variation of the shape energy and applications to spheres and cylinders. Phys. Rev. 39 (10), 5280−5288.